Intensity landscape and the possibility of magic trapping of alkali-metal Rydberg atoms in infrared optical lattices

Turker Topcu and Andrei Derevianko
Department of Physics, University of Nevada, Reno, Nevada 89557, USA
(Received 18 May 2013; published 7 October 2013)

Motivated by compelling advances in manipulating cold Rydberg (Ry) atoms in optical traps, we consider the effect of the large extent of a Ry electron wave function on trapping potentials. We find that, when the Ry orbit lies outside inflection points in the laser intensity landscape, the atom can stably reside in laser intensity maxima. Effectively, the free-electron ac polarizability of the Ry electron is modulated by the intensity landscape and can accept both positive and negative values. We apply these insights to determining the magic wavelengths for Ry-ground-state transitions for alkali-metal atoms trapped in infrared optical lattices. We find magic wavelengths to be around 10 μm with exact values that depend on Ry-state quantum numbers.

DOI: 10.1103/PhysRevA.88.043407 PACS number(s): 37.10.Jk, 32.10.Dk, 32.80.Qk, 32.80.Ee

Magic trapping [1] of cold atoms and molecules is a powerful technique that has recently enabled ultrastable optical lattice clocks [2–4], long-lived quantum memory [5], and precision manipulation of ultracold molecules [6]. When neutral atoms are trapped, their internal energy levels are necessarily perturbed by spatially inhomogeneous trapping fields. For a cold-atomic cloud, typical milli-Kelvin temperatures translate into the 10-MHz trap depths. In other words, as the atom travels about the trap, its energies are modulated at the 10-MHz level with associated coherence times of just 100 ns. If it were not for magic trapping techniques, such decoherences would be prohibitive for the enumerated cold-atom applications. The key idea of magic trapping is the realization that one is interested in differential properties of two levels, such as the clock frequency or a differential phase accumulated by two qubit states. Then if the trapping field affects both levels in the very same way, the differential perturbations vanish. Such engineered traps are commonly referred to as magic. These ideas enabled precision clock spectroscopy at the sub-100-mHz level [3] and second-long coherence times [5], orders of magnitude better than the quoted "nonmagic" values.

Application of magic trapping techniques to Rydberg (Ry) states of alkali-metal atoms has turned out to be challenging. Generic quantum-information protocols involve qubits encoded in hyperfine manifolds of the ground state (GS) and conditional multiqubit dynamics mediated by interactions of Ry states [7–10]. Therefore, the trapping field must be magic both for the GS hyperfine manifolds and for the GS-Ry transition [11]. The first part by itself is a nontrivial problem and has been the subject of several studies [5,12–15]. The GS-Ry transition presents another challenge [11,16–18].

To appreciate the problem, let us first review commonly invoked arguments. In optical fields, the trapping potential is proportional to the ac polarizability $\alpha(\omega)$, leading to trapping potential $U(\mathbf{R}) = -\alpha(\omega)F^2(\mathbf{R})/4$, where F is the local value of the electric field.[1] The GS polarizability is $\alpha_g(\omega) > 0$ when red detuned from atomic resonances, and the atoms are attracted to intensity maxima. On the other hand, a loosely bound Ry electron is nearly "free"; therefore, its polarizability $\alpha_r(\omega) \approx -1/\omega^2$ is negative, and the atoms are pushed towards intensity minima. Then as the GS population is driven to a Ry state during gate operations, an atom experiences a time-varying trapping potential. This causes undesirable motional heating. The resulting decoherence is so severe that experimentalists simply turn off trapping fields during GS-Ry excitations [10,17,18]. This process is also detrimental because this again leads to heating. Such a "pulsed" operation of the trap is the leading heating mechanism in gate experiments with heating rates of $\sim 1\%$ per gate cycle [17]. In addition, there is the problem of scalability: It is impossible to turn off the trapping field at individual trapping sites, therefore, the entire ensemble becomes heated during pulsed trap operations [18].

One way to evade the ac Stark shifts is to use blue-detuned bottle beam traps [19]. Here, the atoms are trapped in intensity minima. Experimentally, such a multitrap setup is arguably more challenging than using optical lattices as discussed below.

Because of the GS-Ry polarizability sign difference, it is usually accepted that magic trapping in red-detuned fields is unattainable (see, however, Ref. [20] for evidence to the contrary). Here we present clear arguments that Ry atoms can, in fact, be attracted to intensity maxima and demonstrate trapping of GS and Ry states in red-detuned magic infrared (IR) lattices.

We start by presenting a qualitative argument (see Fig. 1) that makes the underlying physics transparent. First of all, one realizes that the Ry wave function is spread over long distances that can be comparable to the spatial scale of the laser intensity variations. For example, for a lattice formed by cw lasers of wavelength λ, the laser intensity is spatially modulated with a lattice constant $\lambda/2$: $F^2(z) = F_0^2 \sin^2(kz)$, $k = 2\pi/\lambda$. The Ry orbit is larger than the lattice constant if its principal quantum number is $n > \sqrt{\lambda/(3a_0)}/2$, e.g., $n \gtrsim 100$ for $\lambda = 10$ μm. As a result, the ponderomotive potential experienced by the nearly free electron must be averaged over local field intensities [18,21,22],

$$U(\mathbf{R}) = \frac{1}{4\omega^2} \int d^3r_e |\Psi(\mathbf{r}_e)|^2 F^2(\mathbf{R} + \mathbf{r}_e). \quad (1)$$

[1]Unless specified otherwise, atomic units $|e| = \hbar = m_e \equiv 1$ are used throughout the paper.

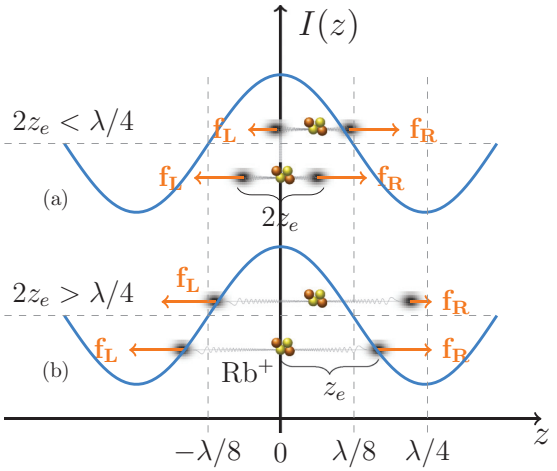

FIG. 1. (Color online) Influence of Ry orbit size on the stability of atomic motion at the 1D lattice antinode for a toy model of a Ry atom. The vertical axis is the laser intensity $I(z)$. The electron cloud is localized in two "lumps". The optical dipole force exerted on each lump is directed towards the nearby intensity minimum and is proportional to the local intensity slope $dI(z)/dz$. When the Ry orbit size is $2z_e < \lambda/4$ [panel (a)], the $\mathbf{f}_R$ and $\mathbf{f}_L$ acting on the localized lumps of electron density pull the atom away from the intensity maximum (unstable equilibrium). When $2z_e > \lambda/4$ [panel (b)], they act as restoring forces with the Ry atom stably resting at the intensity maximum.

Here $\mathbf{R}$ is the position of the atomic core in the laboratory frame, $\mathbf{r}_e$ is the Ry electron coordinate relative to the core, and $|\Psi(\mathbf{r}_e)|^2$ is the Ry electron probability density.

An illustration of the interplay between the Ry orbit size and the lattice constant can be made for a one-dimensional (1D) optical lattice and a toy model of a Ry atom, (see Fig. 1). Here $|\Psi(z_e)|^2$ is localized in two lumps positioned symmetrically (at relative distances $\pm z_e$) about the core. The optical dipole force acting on each lump is transferred to the core by the Coulomb interaction so that the net force on the atom centered at Z reads

$$f_z(Z) = -\frac{1}{8\omega^2}\left(\left.\frac{dF^2}{dz}\right|_{z=Z+z_e} + \left.\frac{dF^2}{dz}\right|_{z=Z-z_e}\right). \quad (2)$$

Because of the symmetry, this force vanishes at the nodes and antinodes of the lattice. In Fig. 1, we investigate the stability of the atomic motion at intensity maxima. It is clear that, for small Ry orbits, the Ry atom is expelled to a nearby antinode as commonly expected. When $2z_e = \lambda/4$, the two lumps sit initially ($Z = 0$) at inflection points in the intensity profile, and the atom experiences no net force regardless of displacement. However, as the size of the Ry orbit is increased ($2z_e > \lambda/4$), the atom stably resides in intensity maxima. As the atom is displaced in some direction, the wave-function lump on the side opposite the displacement experiences a larger dipole-force tug towards the nearby node, resulting in a restoring force.

From this model, we can generalize to an arbitrary three-dimensional laser intensity landscape: *a Ry atom is drawn to intensity maxima if, in an equilibrium position [where* $\nabla I(\mathbf{R}) = 0$*], the bulk of the Ry wave function straddles outside of the nearby surface of inflection points in the intensity landscape, parametrically given by* $\Delta I(\mathbf{r}) = 0$. For example, for a two-dimensional Gaussian intensity cone $I(x,y) = I_0 \exp[-(\rho/\rho_0)^2]$, the radius of the Ry orbit must be greater than $\rho_0(\sqrt{3}-1)/2a_0$. Then a Ry atom can be attracted to the intensity maximum, and its motion can be guided by the beam.

Now we explicitly compute the trapping potential. Integrating over lumps in Eq. (1),

$$U_t(Z) = \frac{F_0^2}{4\omega^2}[\sin^2(kz_e) + \cos(2kz_e)\sin^2(kZ)]. \quad (3)$$

There are two distinct contributions, $U_t(Z) = U_t^0 + U_t^Z \sin^2(kZ)$: The U_t^0 term is a uniform shift across the lattice, and the second contribution is proportional to the standing-wave intensity. The uniform offset does not affect atomic motion as it does not contribute to the force (2). The lattice depth prefactor $U_t^Z = F_0^2/4\omega^2 \cos(2kz_e)$ shows that the atoms are attracted to lattice nodes if $\cos(2kz_e) > 0$, i.e., when $p - 1/4 < 2z_e/\lambda < p + 1/4$, $p = 0,1,2,\ldots$. Otherwise, atoms reside at antinodes. At critical values of $2z_e/\lambda = (p+1/2)/2$, the trapping potential vanishes altogether, and the atom travels through the lattice uninhibited. These observations are consistent with our dipole-force analysis in Fig. 1. As we increase the principal quantum number and the orbit grows larger, the atoms initially stably reside at nodes. Then as $2z_e$ reaches $\lambda/4$, the atoms move freely and then are pushed towards the antinodes. This pattern repeats itself with a further increase in the Ry orbit size.

Having qualitatively understood the nature of various trapping regimes, we now proceed with a rigorous evaluation of trapping potentials for realistic Ry atoms [23]. One starts with the Hamiltonian $(\mathbf{p}_e - \mathbf{A}/c)^2/2$, where $\mathbf{p}_e$ is the electron momentum and $\mathbf{A}$ is the vector potential. Upon expanding the square, we encounter the kinetic-energy term $\mathbf{p}_e \cdot \mathbf{A}$ cross terms and an A^2 contribution. It is the A^2 term in the Coulomb gauge that leads to the ponderomotive potential, and in the lowest-order perturbation theory, we recover Eq. (1). Further discussion of the validity of this approximation can be found in Ref. [24].

Explicitly evaluating the integral (1), we find that the Ry atom potential in a 1D lattice is identical to that of our toy problem in Eq. (3) but with potential shift and depth redefined in terms of expectation values,

$$U_r^Z = \frac{F_0^2}{4\omega^2}\langle nlm|\cos(2kz_e)|nlm\rangle \equiv -\alpha_r^{\rm lsc}(\omega)\frac{F_0^2}{4}, \quad (4)$$

$$U_r^0 = -\frac{\alpha_r^{\rm lsc}(\omega) - \alpha_e(\omega)}{2}\frac{F_0^2}{4} \quad (5)$$

for a Ry state $|nlm\rangle$. Here we introduced the effective intensity landscape-averaged polarizability $\alpha_r^{\rm lsc}(\omega) = -\langle\cos(2kz_e)\rangle/\omega^2$, which unlike the free-electron polarizability $\alpha_e = -1/\omega^2$, can accept both positive and negative values. One can view $\alpha_r^{\rm lsc}$ as landscape-modulated free-electron polarizability as $\alpha_r^{\rm lsc} = \langle\cos(2kz_e)\rangle\alpha_e(\omega)$ and $|\alpha_r^{\rm lsc}(\omega)| \leqslant |\alpha_e(\omega)|$.

The optical potential is $U_r(Z) = U_r^0 + U_r^Z \sin^2(kZ)$. As in our toy model, the potential consists of a term that depends on the position of the atom in the lattice and a uniform offset U_r^0. Note that, without properly accounting for the finite size of the Ry cloud, one would conventionally write $U_r^{\rm conv}(Z) = F_0^2/(4\omega^2)\sin^2(kZ)$. The two potentials, conventional and

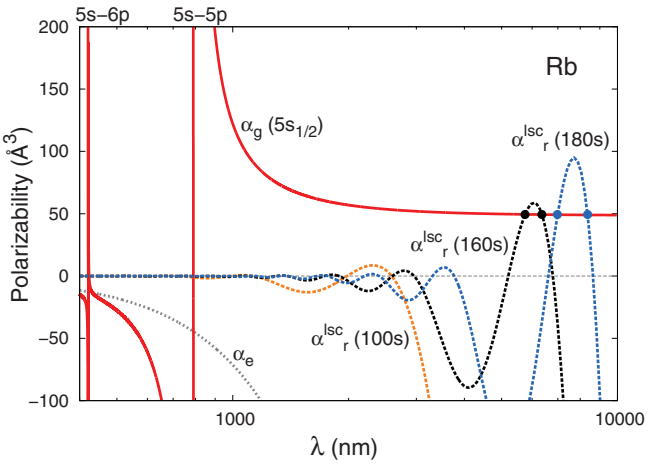

FIG. 2. (Color online) The "landscape-modulated" polarizability $\alpha_r^{\rm lsc}$ for ns states of Rb with $n = 100$ (dashed orange line), 160 (dashed black line), and 180 (dashed blue line). The scalar ground-state polarizability α_g (solid red line) and the free-electron polarizability α_e (dashed gray line) are also shown. The magic wavelengths can be found for all $n \geqslant 154$ in the infrared wavelength range spanning the CO_2 and the frequency-doubled CO_2 laser bands.

ours, are equal only in the limit $\langle r_e\rangle \ll \lambda$ as $U_r^0 \to 0$, and $U_r^Z \to F_0^2/(4\omega^2)$ in this limit. Our potential can support stable equilibrium in lattice antinodes, whereas, the conventional potential does not.

The expectation value of $\cos(2kz_e)$ can be evaluated by expanding $\cos(2kz_e)$ over spherical Bessel functions. For example, for $l = 0$ states,

$$\langle ns|\cos(2kz_e)|ns\rangle = \int_0^\infty dr_e P_{ns}^2(r_e) j_0(2kr_e). \tag{6}$$

Here $P_{ns}(r_e)$ is the radial wave function of the Ry electron; we computed $P_{ns}(r_e)$ using well-known model potentials [25].

Our computed landscape-averaged polarizabilities for several Ry states are shown in Fig. 2. For all the Ry states, $\alpha_r^{\rm lsc}$ is essentially zero at wavelengths below ∼1000 nm and starts oscillating with increasing amplitude before dropping off like $\alpha_e(\omega)$.

By recasting $\alpha_r^{\rm lsc}(\omega) = -[1 - 2\langle\sin^2(kz_e)\rangle]/\omega^2$, one could conclude [23] that $\langle\sin^2(kz_e)\rangle \approx 1/2$ for $\lambda \ll \langle r_e\rangle$ so that $\alpha_r^{\rm lsc} \approx 0$. As λ is increased, kz_e gets smaller, and $\langle\sin^2(kz_e)\rangle \ll 1$, resulting in $\alpha_r^{\rm lsc} \to \alpha_e$. This explains the short- and long-wavelength behavior of $\alpha_r^{\rm lsc}(\omega)$ in Fig. 2. As for the n dependence of $\alpha_r^{\rm lsc}$, one could show, on general grounds, that $\langle\cos(2kz_e)\rangle = f[(n^*)^2 a_0/\lambda]$, where f is some universal function of the effective quantum number n^*. Thus, our discussion is applicable to all Ry atoms.

A possible detrimental effect on the gate fidelity can arise if the wave functions of the Ry atoms trapped at adjacent lattice sites start to overlap. In order to avoid such overlaps, one can fill in the optical lattice by leaving lattice site(s) between trapped atoms empty. Such experimental capabilities have been demonstrated [26]. Furthermore, the Rydberg blockade mechanism, central for the gate operations, relies on the *repulsive* long-range interaction [27]. Penning ionization requires the close approach of two atoms, so the rate is suppressed. As experimentally shown in Ref. [28], since the collisional ionization requires attractive potentials, the Ry states first need to be redistributed (mainly by black-body radiation (BBR) [25]) to populate Ry states that would correlate to attractive molecular potentials at long range. Therefore, decoherence rates due to ionization are limited from above by the BBR-induced decoherences. BBR-induced decoherences were studied in Ref. [17]: At room temperature, the Ry-state lifetime is greater than 0.1 ms for $n > 65$. Thereby, collisional ionization, being the secondary step, is not an issue for Ry gates.

Now since $\alpha_r^{\rm lsc}(\omega)$ can become positive, we show that the GS and Ry potentials can be matched at red-detuned magic wavelengths. For the GS atoms, the trapping potential reads

$$U_g(Z) = -\frac{F_0^2}{4}\alpha_g(\omega)\sin^2(kZ), \tag{7}$$

with the dynamic polarizability (**D** is the dipole operator and E_i's are atomic energy levels),

$$\alpha_g(\omega) = \sum_i \frac{(E_g - E_i)|\langle\psi_g|\mathbf{D}|\psi_i\rangle|^2}{(E_g - E_i)^2 - \omega^2}. \tag{8}$$

We evaluated $\alpha_g(\omega)$ with a high-accuracy procedure [29].

The two spatial parts of Ry and GS potentials match when $U_r^Z = U_g^Z$, which is attained at magic values of laser frequencies ω^* when $\alpha_g(\omega^*) = \alpha_r^{\rm lsc}(\omega^*)$. In Fig. 2, we plot both polarizabilities to search for such magic wavelengths λ^*. We find that, for Rb ns states, the two curves cross for all $n \geqslant 154$ with $\lambda^* \simeq 5600$ nm for $n = 154$. Above this critical value of n, there are at least two values of λ^* (e.g., $\alpha_r^{\rm lsc}$ for the $160s$ and $180s$ states cross twice with the GS polarizability). The number of λ^*'s increases further with increasing n. Table I compiles λ^* for Rb and Na atoms. In addition to the $l = 0$ states, Table I lists λ^* for the $l = 1$ and $l = 2$ states (all $m = 0$).

All these λ^*'s are in the CO_2 and the frequency-doubled CO_2 laser bands. This provides the advantage of individual

TABLE I. Magic wavelengths (nm) for Rydberg states of Na and Rb atoms, $l = 0,1,2$ and $m = 0$.

	$n = 100$			$n = 120$		
	s	p	d	s	p	d
Na		1961 4655	2798 3762		2734 6766	3894 5532
Rb		2022 4421	3016 3401		2750 6525	3942 5301
	$n = 160$			$n = 180$		
	s	p	d	s	p	d
Na	5550 6791	2631 3356 4762 12 134	2820 3312 6792 9961	6923 8695	3269 4305 6006 15 386	3520 4231 8567 12 631
Rb	5755 6363	2735 3132 4714 11 836	2927 3120 6743 9740	6989 8358	3317 4124 5934 15 059	3557 4095 8490 12 402

lattice-site addressing [30]. These wavelengths are far from any resonances, which reduces the photon-scattering rate.

In a trap red detuned from the Rb $5s$-$6p$ resonance but blue detuned from the $5s$-$5p$ resonance, the ground-state polarizability is negative and can be matched to the free-electron polarizability. This allows for a $\lambda^* \approx 432$ nm [10,16]. However, this magic wavelength. being very close to the $5s$-$6p$ resonance, can lead to enhanced photon scattering and heating. Even then, as the landscape averaging reduces the free-electron polarizability employed in Ref. [16], the feasibility of working at that lattice wavelength needs to be revised. Our calculations show (see Fig. 2) that, for $n = 100$ at $\lambda^* \approx 432$ nm, $\alpha_r^{\rm lsc}(\omega^*)/\alpha_e(\omega^*) \approx 3 \times 10^{-3}$, a substantial suppression factor. This reduces the trapping depth, and to make up for the suppression, the laser intensity would need to be increased by a factor of 360.

In quantum gate protocols, such as the controlled-NOT gate, the conditional logic requires driving a π-pulse transition between one of the qubit (ground) states and a Ry state. Although both the qubit and the Ry states see the same trapping potentials in magic lattices, the differential energy shift between these states does not vanish because of the uniform offset term [Eq. (5)]. Drifts in the lattice laser intensity introduce an error $\Delta\omega$ in the Rabi frequency Ω_0 of the GS-Ry transition: $\Omega = \sqrt{\Omega_0^2 + \Delta\omega^2}$. This error in the actual Rabi frequency Ω leads to the fractional error in GS-Ry rotation angle: $\frac{\Delta\phi}{\pi} \sim (\Delta\omega/\Omega_0)^2/2$. For Rb, we estimate this error to be $\frac{\Delta\phi}{\pi} = 25(\frac{\delta I}{I})^2(\frac{1\ \text{MHz}}{\Omega_0})^2(\frac{U}{1\ \text{mK}})^2(\frac{\lambda}{1000\ \text{nm}})^4(\frac{350\ \text{a.u.}}{\alpha_g})^2$, where $\delta I/I$ is the fractional intensity fluctuation and U is the trap depth. For example, when $\delta I/I = 10^{-4}$ for a 0.16-mK-deep trap, $\Omega_0/2\pi = 1$ MHz, and 1000-nm lasers, $\Delta\phi/\pi = 6.5 \times 10^{-9}$. For CO_2 wavelengths, the errors are below 10^{-4}, which is considered to be tolerable [31].

Finally, although we focused on the magic trapping on the Ry-GS transition, simultaneous magic trapping on the qubit transition can also be carried out. For example, techniques employing additional compensating cw traveling laser waves [5] are fully compatible with our proposal. Indeed, since the intensity profile of a traveling wave is uniform in space, it does not affect the spatially varying part of the optical potentials.

We have demonstrated that, although nominally, the Ry-state ac polarizability is essentially that of a free electron and always is negative, the laser intensity landscape can profoundly affect the effective landscape-averaged polarizability and can lead to positive values of polarizability. Landscape averaging depends on the relative size of the Ry orbit and the lattice constant in a nonmonotonic way. A Ry atom can be attracted to intensity maxima. This opens up the possibility for magic trapping of Ry atoms in infrared lattices. The separation between adjacent atoms at these IR wavelengths is comparable to a Ry blockade radius of a few microns, which provides an additional convenience for Ry gate experiments utilizing the dipole blockade mechanism.

We would like to thank M. Lukin, M. Saffman, and E. Tiesinga for discussions. This work was supported by the National Science Foundation under Grants No. PHY-1212482 and No. PHY05-25915.

[1] J. Ye, H. J. Kimble, and H. Katori, Science **320**, 1734 (2008).
[2] M. Takamoto, F.-L. Hong, R. Higashi, and H. Katori, Nature (London) **435**, 321 (2005).
[3] A. D. Ludlow *et al.*, Science **319**, 1805 (2008).
[4] A. Derevianko and H. Katori, Rev. Mod. Phys. **83**, 331 (2011).
[5] A. G. Radnaev, Y. O. Dudin, R. Zhao, H. H. Jen, S. D. Jenkins, A. Kuzmich, and T. A. B. Kennedy, Nat. Phys. **6**, 894 (2010).
[6] B. Neyenhuis, B. Yan, S. A. Moses, J. P. Covey, A. Chotia, A. Petrov, S. Kotochigova, J. Ye, and D. S. Jin, Phys. Rev. Lett. **109**, 230403 (2012).
[7] D. Jaksch, J. I. Cirac, P. Zoller, S. L. Rolston, R. Côté, and M. D. Lukin, Phys. Rev. Lett. **85**, 2208 (2000).
[8] E. Urban, T. A. Johnson, T. Henage, L. Isenhower, D. D. Yavuz, T. G. Walker, and M. Saffman, Nat. Phys. **5**, 110 (2009).
[9] A. Gaëtan, Y. Miroshnychenko, T. Wilk, A. Chotia, M. Viteau, D. Comparat, P. Pillet, A. Browaeys, and P. Grangier, Nat. Phys. **5**, 115 (2009).
[10] M. Saffman, T. Walker, and K. Mølmer, Rev. Mod. Phys. **82**, 2313 (2010).
[11] M. J. Morrison and A. Derevianko, Phys. Rev. A **85**, 033414 (2012).
[12] A. Derevianko, Phys. Rev. Lett. **105**, 033002 (2010).
[13] A. Derevianko, Phys. Rev. A **81**, 051606(R) (2010).
[14] V. V. Flambaum, V. A. Dzuba, and A. Derevianko, Phys. Rev. Lett. **101**, 220801 (2008).
[15] R. Chicireanu, K. D. Nelson, S. Olmschenk, N. Lundblad, A. Derevianko, and J. V. Porto, Phys. Rev. Lett. **106**, 063002 (2011).
[16] M. S. Safronova, C. J. Williams, and C. W. Clark, Phys. Rev. A **67**, 040303(R) (2003).
[17] M. Saffman and T. G. Walker, Phys. Rev. A **72**, 042302 (2005).
[18] S. Zhang, F. Robicheaux, and M. Saffman, Phys. Rev. A **84**, 043408 (2011).
[19] V. V. Ivanov, J. A. Isaacs, M. Saffman, S. A. Kemme, A. R. Ellis, G. R. Brandy, J. R Wendt, G. W. Biedermann, and S. Samora, arXiv:1305.5309.
[20] K. C. Younge, B. Knuffman, S. E. Anderson, and G. Raithel, Phys. Rev. Lett. **104**, 173001 (2010).
[21] S. K. Dutta, J. R. Guest, D. Feldbaum, A. Walz-Flannigan, and G. Raithel, Phys. Rev. Lett. **85**, 5551 (2000).
[22] K. C. Younge, S. E. Anderson, and G. Raithel, New J. Phys. **12**, 023031 (2010).
[23] V. D. Ovsiannikov, A. Derevianko, and K. Gibble, Phys. Rev. Lett. **107**, 093003 (2011).
[24] T. Topcu and A. Derevianko, arXiv:1308.0573.
[25] T. F. Gallagher, *Rydberg Atoms* (Cambridge University Press, Cambridge, UK, 2005).
[26] I. Bloch, J. Dalibard, and S. Nascimbene, Nat. Phys. **8**, 267 (2012).

[27] M. D. Lukin, M. Fleischhauer, R. Cote, L. M. Duan, D. Jaksch, J. I. Cirac, and P. Zoller, Phys. Rev. Lett. **87**, 037901 (2001).

[28] T. Amthor, M. Reetz-Lamour, C. Giese, and M. Weidemüller, Phys. Rev. A **76**, 054702 (2007).

[29] A. Derevianko, W. R. Johnson, M. S. Safronova, and J. F. Babb, Phys. Rev. Lett. **82**, 3589 (1999).

[30] R. Scheunemann, F. S. Cataliotti, T. W. Hänsch, and M. Weitz, Phys. Rev. A **62**, 051801(R) (2000).

[31] E. Knill, Nature (London) **434**, 39 (2005).